GA–A22598

MODELING OF 110 GHz ELECTRON CYCLOTRON WAVE PROPAGATION AND ABSORPTION ON DIII–D

by

Y.R. LIN-LIU, T.C. LUCE, S.C. CHIU,
R.L. MILLER, and R. PRATER

APRIL 1997

GA–A22598

MODELING OF 110 GHz ELECTRON CYCLOTRON WAVE PROPAGATION AND ABSORPTION ON DIII–D

by

Y.R. LIN-LIU, T.C. LUCE, S.C. CHIU,
R.L. MILLER, and R. PRATER

This is a preprint of a paper presented at the 12th Topical Conference on Radio Frequency Power in Plasmas, April 1–3, 1997, Savannah, Georgia, and to be printed in the *Proceedings.*

Work supported by
U.S. Department of Energy
Contract DE-AC03-89ER51114

GENERAL ATOMICS PROJECT 3466
APRIL 1997

Modeling of 110 GHz Electron Cyclotron Wave Propagation and Absorption on DIII–D

Y.R. Lin-Liu, T.C. Luce, S.C. Chiu, R.L. Miller, and R. Prater

General Atomics, San Diego, California 92186

Abstract. Warm plasma refraction effects on wave propagation and absorption are examined in the context of a slab model in the parameter regime of interest to the upcoming 110 GHz electron cyclotron heating and current drive experiments on DIII–D.

In modeling electron cyclotron (EC) waves for heating (ECH) and current drive (ECCD) applications, the standard approach describes wave propagation using geometric optic ray tracing with cold plasma dispersion and wave absorption using a relativistic warm plasma expression. However, recent vertical O–mode transmission measurements on Tore Supra [1] indicate that wave trajectories near the fundamental resonance frequency can significantly deviate from predictions of cold plasma analysis. The experimental results were attributed to warm plasma refraction effects caused by the anomalous dispersion associated with wave-particle resonance [2,3]. In this work, we examine the anomalous dispersion using a weakly relativistic dielectric model of Matsuda and Hsu [4]. We assess the impact of the warm plasma refraction effects on wave propagation and absorption using a slab model. Our attention focuses on the parameter regime directly relevant to the upcoming 110 GHz ECH and ECCD experiments on DIII–D.

The goal of the ECH and ECCD experiments on DIII–D is to demonstrate the capability of localized heating and current drive for pressure and current profile control in the advanced tokamak operational regime. In the new DIII–D ECH system, 110 GHz EC waves with X–mode polarization are launched from an upper low-field side port. The microwave beam is injected 19° off normal for current drive applications, and it can be steered poloidally to provide power deposition from the center to the upper outer edge of the plasma. For details of the ECH system see Callis *et al.* in these Proceedings. The major and minor radii of DIII–D are, respectively, $R_0 = 1.7$ m and $a = 0.6$ m. The nominal magnetic field is $B_0 = 2.0$ T. The plasma parameter regime of interest in the near-term experiments ranges from $n_e T_e = 0.5 - 1.5$ (10^{20}m^{-3} keV).

We examine the anomalous dispersion using the weakly relativistic dielectric model of Matsuda and Hsu. The model includes the leading order correction terms of finite Larmor radius (FLR) effects consistently up to the third harmonic in resonance denominators. The dispersion relation is expressed as a polynomial equation in $n_\perp^2$, to be solved iteratively starting with an initial guess of the cold plasma solution. We have successfully benchmarked our numerical results with those of the ‘‘reduced weakly relativistic’’ model [5], which is based on the well known Shkarofsky's approximations.

In Fig. 1 we show the real (imaginary) part of the perpendicular refractive index of the X–mode as a function of ω/ω_c for given $n_{||}$ with $T_e = 5$ keV and $n_e = 0.3\times10^{20}$ m^{-3}, corresponding to $(\omega_p/\omega)^2 = 0.2$. Note that near $\omega/\omega_c \approx 2.0$ the dispersion relation exhibits anomalous behavior and shows characteristics of a back-to-back resonance and cutoff. In the case of $n_{||} = 0$, modification of the real part of the refractive index due to warm plasma effects is appreciable, but damping is negligible in the region of $\omega/\omega_c \geq 2$. For oblique incidence, the magnitude of the refractive index anomaly decreases as $n_{||}$ increases. Moreover, finite $n_{||}$ introduces Doppler shift of the resonance frequency which broadens the absorption profile and gives rise to wave damping on the lower field side of the resonance layer. We have also examined the anomalous dispersion at different electron densities and temperatures. The magnitude of the refractive index anomaly is approximately proportional to density and is insensitive to temperature.

We now use a slab model to assess the impact of the anomalous dispersion on wave propagation and absorption. In this slab model, inhomogeneity is taken to be along the x-direction. The magnetic field is assumed to be straight and has the form of $\vec{B}(x) = B_0/(1 + x/R_0)\hat{z}$. The profiles of temperature and density are taken to be constant. The microwave beam is considered as a superposition of plane waves in the z-direction and its $x - y$ dependence is described by an eikonal approximation. As a result of the simplified geometry $n_{||} = n_z$ and n_y are constants specified by the launch condition; and $n_x^2 + n_y^2 = n_\perp'^2(x)$ where $n_\perp'$ is taken to be the

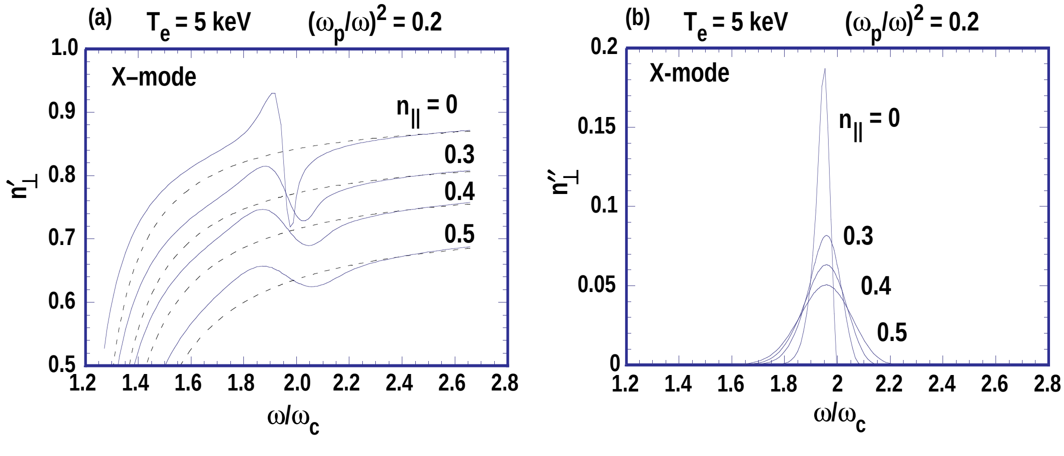

FIGURE 1. X–mode real and imaginary part of perpendicular refractive index $n_\perp$ as a function of ω/ω_c for different $n_{||}$, $(\omega_p/\omega)^2 = 0.2$, and $T_e = 5$ keV.

real part of the solution for appropriate wave mode of the warm plasma dispersion [3]. The ray trajectory in the $x-y$ plane satisfies the simple equations: $dx/d\ell_\mathrm{p} = n_x/n'_\perp$ and $dy/d\ell_\mathrm{p} = n_y/n'_\perp$, where $d\ell_\mathrm{p}^2 = dx^2 + dy^2$. The fraction of power absorbed along the ray path is given by $f = 1 - \exp(-2\int_0^{\ell_\mathrm{p}} \vec{k}''_\perp \cdot d\vec{\ell}_p)$, where $k''_\perp$ is the imaginary part of the perpendicular wave vector.

By making use of $n_x^2 + n_y^2 = n'^2_\perp(x)$ and noticing the dependence of $n'_\perp$ on $\omega/\omega_\mathrm{c}(x)$ as shown in Fig. 1(a), we can see why the warm plasma refraction effects will be maximized in a nearly vertical launch. In this case, n_y (n_y is a constant) $\approx n'_\perp >> n_x$ The outside launched waves which could have reached the resonance layer according to the cold plasma theory will encounter an ‘‘apparent’’ cutoff, $n_x(x) = 0$, introduced by the anomalous dispersion at the lower field side of the resonance layer, well before they see the cold plasma cutoff. Furthermore, in the case of $n_\parallel \approx 0$, wave damping in that anomalous region is negligible and a nearly complete reflection of the wave from the resonance layer becomes possible [see Fig. 2(a)]. We may define a critical ‘‘poloidal’’ injection angle θ_c^0 (measured from the vertical direction) at which the fraction of power absorbed $f < 63.2\%$, *i.e.*, the effective optical depth is less than 1. In Fig. 3, we show that θ_c^0 as a function of $n_\parallel$ for a 5 keV plasma of two different densities corresponding to $(\omega_\mathrm{p}/\omega)^2 = 0.067$ and 0.2 ($n_\mathrm{e} = 0.1$ and 0.3×10^{20} m^{-3}). Since the value of θ_c^0 is determined mainly by the magnitude the refractive index anomaly near the resonance, θ_c^0 is expected to be a weak function of temperature. In practical ECCD launch configurations, the poloidal injection angle θ is usually sufficiently larger than θ_c^0. One expects that impact of the warm plasma effects would be less

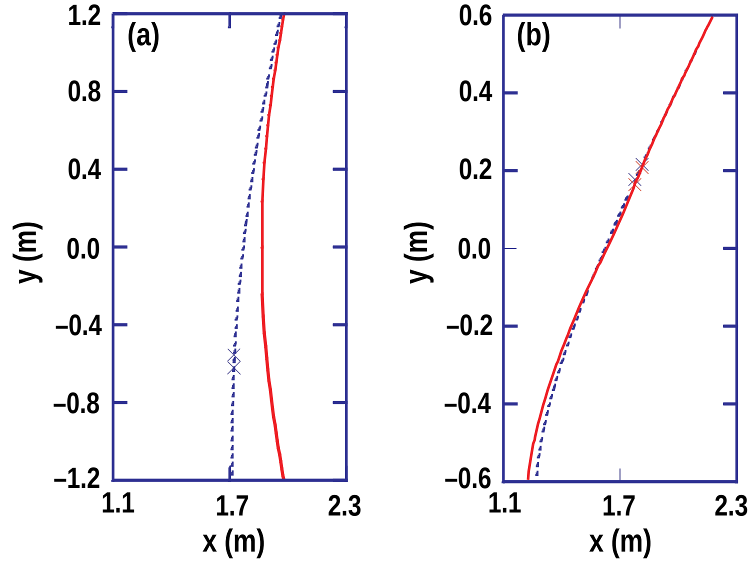

FIGURE 2. Ray trajectories of the slab model from warm-plasma (solid line) and cold-plasma (dotted line) analyses; crosses mark locations at which the effective optic depths are 1 and 5, respectively; $(\omega_\mathrm{p}/\omega)^2 = 0.2$, $T_\mathrm{e} = 5$ keV, injection angles: (a) $\theta = 15^\circ$, $\phi = 0^\circ$ ($n_\parallel = 0.0$), (b) $\theta = 45^\circ$, $\phi = 23.5^\circ$ ($n_\parallel = 0.4$).

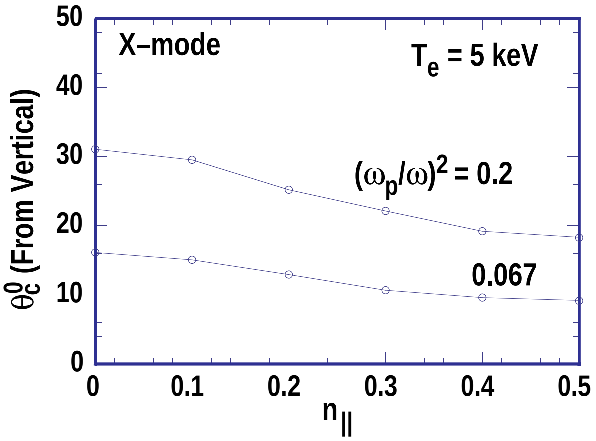

FIGURE 3. The $n_{||}$ dependence of critical poloidal injection angle θ_c^0 for a 5 keV plasma at two different densities.

profound. In Fig. 2(b), we compared ray trajectories from the warm- and cold-plasma analyses for a plasma of $T_e = 5$ keV and $n_e = 0.3 \times 10^{20}$ m^{-3} and a launch configuration ($\theta = 45^\circ$ and $\phi = 23.5^\circ$) which simulates that of DIII–D. Along the trajectories locations at which the effective optical depths 1 and 5, respectively, are marked by crosses. By comparing the two trajectories, ray refraction due to the warm plasma effects behaves expectedly according to the anomalous dispersion, but is barely visible. The refraction effects would alter the power deposition profile toward the low field side in comparison with predictions from the cold plasma analysis. In the case examined here, the difference is very small and is on the order of a few wavelengths.

In summary, we have used a slab model to examine the warm plasma refraction effects on wave propagation and absorption in the parameter regime of interest in upcoming 110 GHz ECH and ECCD experiments on DIII–D. The model study indicates that refraction effects would be significant in the case of nearly vertical launch with $n_{||}$ close to zero. For the practical ECCD launch configuration with large poloidal injection angles, refraction effects appear to be unimportant.

This is a report of work sponsored by the U.S. Department of Energy under Contract DE-AC03-89ER51114.

REFERENCES

1. J.L. Segui *et al.*, ‘‘An overview of ECA results in Tore Supra,’’ in *Proc. 9th Joint Workshop on ECE and ECH*, Borrego Springs, California, 1995, p. 223.
2. S. Pesic, Europhys. Lett. **35**, 349 (1996).
3. E. Westerhof, ‘‘Wave propagation through an electron cyclotron resonance layer,’’ FOM-Instituut voor Plasmafysica Rijnhuizen Report (1996).
4. K. Matsuda and J.Y. Hsu, Phys. Fluids B **3**, 414 (1991).
5. H. Binslev, ‘‘Relativistic effects in millimeter wave applications in magnetically confined plasmas,’’ in *Proc. 9th Joint Workshop on ECE and ECH*, Borrego Springs, California, 1995, p. 585.